DSDU-Net: Segmentation of Brain Tumor Subregions with Depthwise Separable Dense U-NET

V Nehru (nehruveerabatheran@gmail.com)
Vel Tech Multitech Dr.Rangarajan Dr.Sakunthala Engineering College

Prabhu V
Vel Tech Multitech Dr.Rangarajan Dr.Sakunthala Engineering College

Research Article

Keywords: Brain Tumor Segmentation, Depthwise Separable Convolutional Networks, Whole Tumor (WT), Tumor Core (TC), Enhancing Tumor (ET)

Posted Date: May 26th, 2022

DOI: https://doi.org/10.21203/rs.3.rs-1689340/v1

DSDU-Net: Segmentation of Brain Tumor Subregions with Depthwise Separable Dense U-NET

[1*]*Nehru V,* [2*] *Prabhu. V,*

[1]*Assistant Professor, Department of Computer Science and Engineering,Vel Tech Multitech Dr.Rangarajan Dr.Sakunthala Engineering College, Chennai-600062, Tamil Nadu, India;*
[2]*Associate Professor, Department of Electronics and Communication Engineering,Vel Tech Multitech Dr.Rangarajan Dr.Sakunthala Engineering College, Chennai-600062, Tamil Nadu, India;*
Email nehruveerabatheran@gmail.com[1,], prabhuv@veltechmultitech.org [2],*

ABSTRACT
Brain tumors are one of the most dangerous medical conditions. The dispersed extremities and non-uniform structure of the tumors are the basis of why techniques of traditional segmentation have grown to be inefficient. Magnetic Resonance Imaging (MRI) is one of the most widely used scanning procedures for tumors. However, to ameliorate the survival rate, the detection of tumors alone does not suffice, and there are other effective procedures. One of the most pivotal procedures for diagnosing the condition is the process of the brain tumor segmentation is a laborious and cumbersome process. As a result, a Deep Learning (DL) based solution is used to extract tumor subregions like Enhancing Tumor (ET), Tumor Core (TC), and Whole Tumor (WT). The proposed model involves novel DSDU-Net: Depth-wise Separable Dense U-NET (DSDU-NET) that precise outputs are acquired by retaining the low-level features. In the preprocessing stage, a methodology called Multi-Scale Patch extraction is used to segregate tumor regions, and a grouping of Gaussian Filter, Unsharp Masking, and Histogram Equalization is carried out on the data set to get significantly better performance.The proposed DSDU-NET network performed better in terms of performance, specificity, sensitivity, dice similarity index, and Hausdorff Distance for segmented image sub-regions when validated on BraTS 2018 and 2019 datasources When particularly in comparison to other models.

Keywords : *Brain Tumor Segmentation; Depthwise Separable Convolutional Networks; Whole Tumor (WT); Tumor Core (TC); Enhancing Tumor (ET)*

1. INTRODUCTION

Gliomas and braintumors are the leading causes of death in several countries. Two processes play the most significant role in treating brain tumors, diagnostics and growth prediction, automatic segmentation, and classification of medical images. The early diagnosis of brain tumors infers a quicker reaction to treatment, which ensures an improved survival rate of patients. In large medical image databases, the classification and location of brain tumors performed regularly as a clinical procedure by manual methods proves to have a high cost in both time and effort (Díaz-Pernas et al, 2021). A brain tumor is found to be a pervading reason for death due to cancer. More than 70000 citizens have tumors in their brains (20% malignant and 80% benign) in the USA. In 2020, around 18020 deaths due to malignant

tumors of the brain and 23890 malignant brain tumors were estimated by the American Cancer Society (ACS) for brain tumors. Therefore, Tumor treatment planning and diagnosis, precise and accurate quantitative methods, and segmentation of brain tumors are necessary. Hence, the automatic indication, position, and classification procedures are advantageous and valuable (Nassar et al.,2021). Tumors are divided into two categories: primary & secondary. Tumors that develop from the brain cells are called primary brain tumors, and secondary tumors are formed by metastasizing into the brain from various other parts of the body. Gliomas develop from the brain's glial cells, which is the most occurring type. Gliomas are graded from grade 1 (lowest grade) to grade 4 (highest grade) relying on histopathologic features such as cytological atypia, anaplasia, mitotic activity, microvascular proliferation, and necrosis, according to the World Health Organization (WHO). Grades 1 & 2 are also known as Low-Grade-Gliomas (LGG), and they are prone to developing slowly. High-Grade-Gliomas (HGG) is another name given to Grade III and IV, which are fierce and cancerous (Wu et al., 2020) and generally require surgery and/or radiotherapy, having ominous survival prediction (Myronenko, 2019).

The MRI is a non-intraoperative and extensively favored method utilized by radiologists to provide complicated and detail-oriented brain images. Hence, it is widely utilized for the preliminary characterization and prognosis of tumors. In addition, the MRI could be used to segment brain tumors and provide information about the tumor, such as its location for biopsy sampling, which leads to tumor grading by a pathologist and its size and shape. During acquisition, an MRI produces several image slices (hundreds) in 2D that have high contrast for soft tissues without ionizing radiation. Generally, four significant methodologies are used in MRI diagnosis. They are as follows: T1-weighted MRI (T1), Fluid-Attenuated Inversion Recovery (FLAIR), T1-weighted contrast-enhanced MRI (T1-CE), and T2-weighted MRI (T2). Every individual modality provides scans that have various tissue contrasts; therefore, some modality is further complementary to explore a particular type of tissue compared to others. Different glioma tissues are contemplated by different sequences of the MRI (Zawish et al., 2019). T1 images are predominantly employed to study healthy tissues. T2 modality is more applicable to indicate boundaries of regions of edema. T1-CE sequence accentuates borders of tumor. It is appropriate for the observation of the tumor core and its active components. FLAIR modality aids in indicating the regions of swelling in CSF. T1-Ce is sufficient if the goal is to process brain tumor location and classification using MRI (Díaz-Pernas et al, 2021). Multi-modal MRIs provide additional information for tumor analysis because they can reveal glioma’s sub-regions.Nevertheless, manual depiction is not very efficient in most medical and clinical progress as it is considered to be slow-moving and burdensome, which is also influenced by the equivocation of accurate interpretations (Luo et al., 2021).

Various methods have been explored for brain tumor segmentation throughout the literature. These methodologies can be classified as deep learning methods (Serte et al., 2020). and traditional methods (generative or discriminative).Generative methods utilize atlases of healthy tissues (atlas-based models) to fragment the unspecified tumor segments on test images, with the favor of previous knowledge, e.g., the spatial extent and location of healthy tissues. For volume pixel categorization, it uses back-end probabilities, as well as image registration for tumor segmentation (Naser & Deen, 2020).Discriminative methods seek to

extract discriminative features; subsequently, classification is performed by a classifier.Discriminative models, including SVM and random forests, classify voxels using imaging features obtained from the MRI instead of accurate MRI data.

There are certain limitations associated with the works done previously. They are:

- Present generative methods have computationally expensive registration tasks, which are considered an impediment. Further, the in-built atlas might not be able to showcase the population of images.
- Present discriminative methodologies have their limitations from lack of features that could showcase brain cancer, which leads to lesser accuracy of prediction.

Since segmentation of tumors manually is a tedious and slow-paced process, automatic segmentation employing the Computer-Aided Diagnostic (CAD) system is utilized to assist the radiologists in performing the task of segmentation of brain tumors. (Nassar et al.,2021). Glioma segmentation and the abnormal tissues surrounding them based on MRI facilitates a physician's observation of the outer structure of each malignant cell of a patient's glioma and the physician's assessment and post-treatment based on imaging. As a result, segmenting the glioma is considered the first step in the MRI-based examination. (Zawish et al., 2019)

This paper proposes a novel U-Net-based design. It employs diverse U-net blocks in order to detain data at various resolutions of long-distance spatial information. Extraction and utilization of sufficient features have been done by upsampling feature maps with varying resolutions and assuming that it is easier to learn and process similar features. Furthermore, Depthwise separable convolutional networks have been used rather than conventional 3D CNN to reduce computational costs. The following are the highlights of our accomplishments in this study:

1. The model was designed using DSDU-Nets and multiscale patches that extract features by upsampling feature maps at different resolutions.
2. Obtaining lengthy spatial data at various resolutions using DenseU-Net blocks. Time and space complexity has been reduced by using separable convolutional neural networks.
3. Final results are obtained from comparisons of BRATS Datasets.

Structure of the paper:

The remaining part has been organized as Section 2 summarises the existing DL models of brain tumor-segmentation. Third section introduces methodologies. The dataset and performance metrics are discussed in fourth section. Section 5 summarises the findings and analysis. At the end of the paper, Section 6 outlines concluding remarks.

2. RELATED WORKS

Several studies have been conducted over the years for brain tumor sub-regions segmentation. For example, in a paper by Myronenko et al., they proposed a CNN architecture predicated on the encoder-decoder framework with asymmetrical components. A larger encoder is in charge of FE, while a smaller decoder is in charge of segmentation mask reconstruction. (Myronenko, 2019).

In this paper, the features are extracted and classifies in skin lesions using support vector machines based on AlexNet and VGG-16 models. It obtained area of curve values of 98% and 97%. (Almezhghwi et al., 2021)

Isensee F. et al. projected a 3D U-Net framework whose encoder section was similar to the conventional CNN classification. U-Net recovers the spatial information lost during information aggregation by CNN through the decoder. Through skip connections, essential data from 'U' base is combined with higher resolution feature maps acquired from encoder. (Myronenko, 2019)

McKinley introduced a new set of classifiers, (McKinley et al., 2019) This model was based on DeepSCAN. The architecture that consisted of several blocks of densely connected dilated convolutions was trained with the help of a novel loss function. Another work done by Zhou, C. et al. had explained about the use of several deep learning models for capturing attentive and contextual information. The predictions made from these models were eventually used for obtaining precise results in Segmentation. Thus, the problem of overfitting in Segmentation was significantly decreased (Zhou et al., 2019). Bacanin et al. In this paper, an automatic image classification system is developed to classify glioma brain tumor. the proposed convolutional neural network model implies hyperparameters' optimization using modified firefly algorithm to get optimal solution. (Bacanin et al., 2021)

A default end-to-end multi-label learning for dense volumetric Segmentation was conducted by Z. Luo et al. A 4-channel input with a concatenated set of images from several imaging modalities is given to the model. At the heart of the 3D segmentation model is an HDC-Net that essentially works with 2D convolutions (Luo et al., 2021). A multi-planar ConvNet model was also introduced by Banerjee S et al. for sub-regions segmentation automatically. The structure of the tumor body was better analyzed using spatial max pooling and unspooling layers. Upsampling has been used for minimizing errors during Segmentation around the tumor boundary (Banerjee & Mitra, 2020). Two-block cascaded U-Net with variational autoencoder for Segmentation as an attempt at better Segmentation (Jiang et al., 2020).

A variation of 3D CNN, CANet was proposed by Pei L et al., Segmentation of brain tumors. Its front end of CANet was used to extract HD features, and linear regression was used to make a complete survival prediction (Pei et al., 2020b). A 3D unit structure with several hyperparameters was introduced by Feng et al., which consisted of pre-processing, patch extraction, and training of several CNN models. Each model was deployed for volume prediction and final ensembling (Feng et al., 2020). Oday Ali Hassen et al. introduced a model that uses level set segmentation and Artificial Bee Colony optimization to satisfy parameters that could help detect brain tumors (Ali Hassen et al., 2021). Segmentation of brain tumors was also achieved by Bayesian active learning and GAN networks by Alshehhi, R. et al., (Alshehhi & Alshehhi, 2021).

A model based on multi-scale prediction with 3D U-Net where feature extraction takes place in the encoder part of the network and downsampling by ReLU was proposed by Chen M et al. (Chen et al., 2020). Muti-resolution features derived by the decoder were then aggregated to give the final segmentation result. Hamghalam M. et al. proposed a model that segmented

was fed with MR volume, $I \in R^{H \times W \times D}$, based on labels $S \in \{1, 2, ..., c\}^{H \times W \times D}$, in which outcomes are given by c. H stands for spatial height, W for spatial width and D for spatial depth (Hamghalam et al., 2020). A model that segmented brain tumors was also created using multimodal 3D magnetic resonance (MR) volumes made from synthetic images.3D FCN was used for segmentation in a model developed by Hamghalam M et al., (Kim et al., 2020). Li X and colleagues propose using a multi-levelcascaded network for precise brain tumor segmentation in a separate study.Their network architecture consisted of three major components: a 3DU-Net architecture with deep supervisions, as well as a multi-levelcascaded network. (Li et al., 2020).

Summary:

Existing deep learning methods for brain tumor's segmentation that use CNN incur significant computational and training costs. The selection of the correct number of neurons per layer and the ideal number of total layers is a frequently debated problem (Nassar et al., 2021). Although several models show satisfactory overall performance, not many models have achieved peak accuracies on segmentation tasks (Luo et al., 2021). Furthermore, most methods are time-consuming and only improve the results slightly (Jiang et al., 2020). A novel method that successfully overcomes this limitation has been proposed in this paper.

3. Methods and Materials

3.1 Overview

The proposed deep learning method has three stages: First, Pre-processing using image processing methods, patch extraction, and segmentation into corresponding tumor sub-region. Gaussian filters have been used to remove noise and to smooth the image. Second, brightness enhancement by normalization of image intensity distribution is done using histogram equalization, and edge enhancement is improved by unsharp masking. Third, corruption of images due to magnetic fields is corrected by bias removal. Further, N4ITK is used for intensity correction. Finally, normalization is done as the last step in pre-processing.

Pre-processing is followed by multi-patch extraction. First, the images are resized, and the tumor's portion is extracted from the MRI image. The patch extracted images are then fed into the Depthwise Separable CNN model combined with Dense U-Net. This portion of the network isolates the different subregions in the tumor and gives the output in ET, TC, and WT.

3.2 BraTS Database

BraTS(BrainTumorSegmentation)database contains MRI-images of brain-tumors acquired from-various imaging equipment and under different imaging protocols. They were collected from several health centers under standard clinical conditions. The images were of varying qualities and segmented manually on the scale from 1 to 4 based on the same annotation protocol. Three sub-regions were used for evaluation purposes -

a) The active tumor or the tumor that is enhancing (ET). This section describes the areas where contrast discharge occurs, indicating a breach in the blood-brain obstruction. (Pei et al., 2020a).

b) Tumor core (TC) comprises necrotic tissues as well. The tumor core is the part that is most commonly resected during surgeries.

c) The whole tumor (WT), which is the complete tumor. This label is the union of all labels in the dataset. Since the invaded tissue also consists of tumor cells and edema, it is also taken as a section in WT.

The parts of the active tumor that show hyper-intensity in T1Gd compared with T1 and when compared with 'healthy' whitematter tissue in T1Gd are classified. The tumor substance that is commonly resected is usually denoted by TC. The enhancing tumor, necrotic, i.e., fluid-filled, and non-enhancing section of tumor entail the tumor core. Necrotic and the non-enhancing tumor core appearance is usually hypo-intense in T1-Gd in comparison to T1. The whole tumor entails TC and ET, i.e., peritumoral edematous/invaded tissue (ED). This is usually highlighted in T2-FLAIR by a hyperintense signal. The ground annotations of these images were created by several experts and were then approved by experts in the domain. The annotation styles were slightly different for each rater through a particular and detailed annotation protocol was described to the institutions from where the data was acquired. As a result, a domain specialist of over 15 years experience in neuroradiology was appointed to review the final labels for compliance and consistency with the annotation protocol. (Bakas al., 2018).

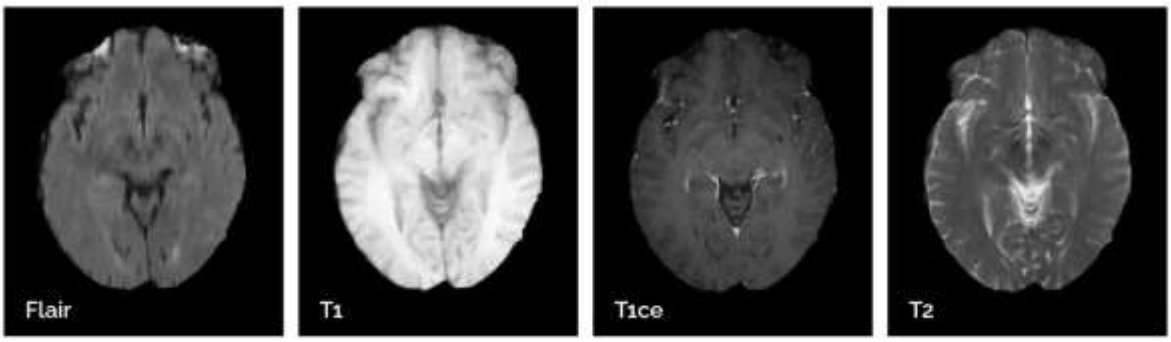

Figure 1. Samples from the BRATS 2018 dataset. Flair, T1, T1ce, T2 (From left to right)

The current architecture has been assessed using the standards of BraTS of 2018 and 2019. The dataset contains MR scans obtained from 4 modalities – T2, T1, T1ce, and Flair, and their respective segmentation maps. Segmentation is done with four labels - 1, 2, 4, and 0-non-enhancing tumor core (NCR/NET), peritumoral edema (ED), and ET. For validation, MRI data were taken from datasets.(comparable to the training dataset but without segmentation.) They were placed in same location that used the same MR volume matrix (X, Y, Z = 240 × 240 × 155) [15]. The BraTS 2018 dataset consisted of 285 images, while the BraTS 2019 dataset consists of 355 cases (Zhao et al., 2020).

3.3 Pre-processing

Better quality images are obtained by pre-processing the data set using Unsharp Masking, Histogram Equalization, and Gaussian Filter. Normalization, bias removal, and standardization are also carried out before the data is sent for segmentation. Bias field created due to the inhomogeneity of magnetic fields is removed by bias removal. This signal with a low frequency degrades MRI images and distorts frequencies of a higher range. The N4ITK

algorithm is used for correction, which is an extension of N3. The pixel intensity range is changed during normalization. The mathematical representation of this process is given below.

$$I_{new} = \frac{(I - Min)(Max_{new} - Min_{new})}{Max - Min} + Min_{new} \quad (1)$$

where ,

I_{new} represents new-pixel-value, Max reresents old-maximum-value, Min:represents old-minimum-value, I represent old pixel value, Max_{new} represents new maximum value, and Min_{new} represents new minimum value.

$$I_{new} = \frac{I - \mu}{\sigma} \quad (2)$$

where, I_{new} stands for new-pixel-value, μ denotes image-set average and σ is the image set standarddeviation(SD).

Patches of N×N are also normalized after normalization of individual slides before testing and training. This is done so that they maintain zero mean and unit variance after pre-processing has been completed.

3.4 Multiscale patch extraction

Images in the dataset are extracted in patches. The windows are of dimensions w × h with s as the stride for both original and resized images. The patch size is set to 224 x 224 since the DenseUNet model. The range of extracted clusters from data with a size of H × W is represented as follows:

$$N = \left(\left\lfloor\frac{W-w}{s}\right\rfloor + 1\right) \times \left(\left\lfloor\frac{H-h}{s}\right\rfloor + 1\right) \quad (3)$$

Here$\lfloor N \rfloor$represents rounded-down. Also,intensities are again set to unit variance, and zero mean. Two data augmentation techniques that raise the diversity and size of the dataset have been introduced. This also helps in resolving the problem of overfitting. Each patch is converted into 8 patches by amalgamating $K.\frac{\pi}{2}$rotations, Where $K = \{0,1,2,3,\}$. Vertical reflections may or may not be present at this step. The patches are also processed with perturbations. Thus, we have about 259200 patches ready for training by the model, which allows it to learn mirroring invariant, and rotation invariant representation of images.

3.5. Depthwise Separable CNN

The Depthwise Separable CNN is formed from two convolutions - depthwise and pointwise. A convolution is carried out on every input volume in a depthwise convolution while the depthwise convolution outputs are merged using the pointwise convolutions (Alalwan et al., 2021). Depthwise separable convolution has been utilized here rather than the traditionally used convolutional networks since they reduce computational costs. Two filters have been used to break down a traditional convolution - filters are first applied to each channel and then a 1 × 1 × 1 filter to combine all the output feature maps point-by-point. These operations are performed on the assumptions that the input features are of shape D × D × D, no. of input

and output channels is denoted as M and N, and K × K × K denotes size of convolutional kernel. When N convolution kernels tracks the data in M streams in a conventional convolution, feature maps of M×N are generated.. Eventually, feature maps (M) are superimposed with their corresponding maps, and a feature map is obtained. Thus, the N output channels that are required are obtained. This process is depicted in the figure below. The cost of computation of the process is: K × K × M × N × D × D

M feature maps are created when different filters are applied to each channel in the depth-wise separable convolution. The feature maps(M) are then point-by-point linearly combined by 1 × 1 filters. The number of N output channels that are required is achieved. Figure 6 depicts the procedure. The process's computational cost is :

$$K \times K \times M \times D \times D + 1 \times 1 \times M \times D \times D$$

We get ( ) by using ( ) dividing ( ):

$$\frac{K \times K \times M \times D \times D + 1 \times 1 \times M \times D \times D}{K \times K \times M \times N \times D \times D} = \underline{1/N + 1/K3}$$

The kernel size is traditionally 3 × 3 × 3and number of available channels N is 16, 32, 64, 128, etc. Decrease in the computational costs can be seen as well after this process (Peng et al., 2019).

3.6. Dense U-Net

The DenseUNet architecture is composed of repeated blocks of DenseNet networks. Each of these blocks has varying output dimensions with links connecting each succesive layer. Maximum flow of information is achieved by these connections between each block that improves convergence to an ideal solution. We make the assumption that

$$I \in R^{n \times (224 \times 224) \times cn}$$

Ground-truth classifications for training images (for 224224 input volume) are as follows:

$$Y \in R^{n \times (224 \times 224) \times 1}$$

The input batch size is denoted by n, and the channel is represented by the last dimensioncn. A class c can be assigned to each pixel (i;j;k) (brain,tumor and background), i.e., $Y_{ijk} = c$; and thus segmentation for brain and tumor by the DenseUNet is;

$$X = f(I, \Theta); X \in R^{n \times (224 \times 224) \times 64}$$
$$\hat{y} = f(X, \theta), \hat{y} \in R^{n \times (224 \times 224) \times 3}$$

The pixel-wise outcomes for the input data I are denoted by X, and the final up-sampling layer's (Fifth layer; refer Figure. 2) feature vector is denoted by Y. Let theta represents model parameters such as convolution weights and bias conditions of ReLU. Upsampling and transition blocks, activation layers, batch normalization layers with pointwise and depthwise convolutional layers are among the layers in the model. The transition block decreases the number of characteristic vectors. BN layer, 1x1 convolution layer & convolution layer of stride 2 make up the transition block. Expansion of feature maps was prevented by setting the compression factor to 0.5. A bilinear interpolation layer makes up the upsampling blocks. As a result, a set of low-level functionalities, such as UNet connections and a 3x3 convolutional

layer, are added from dense blocks exact reverse of current block. Broader and deeper networks are created using the BN layer, contributing to the network's success. A rectified linear unit (ReLU) layer is implemented by the activation layer. These layers are executed after each convolutional layer. The ReLU layers ensure optimization of the model and enhancement of its performance.

3.7. Loss function

Precise learning of parameters and features from the images in the dataset, function loss is minimised. This function was used as weighted-crossentropy and is represented below:

$$L(y, \hat{y}) = -\frac{1}{N} \sum_{i=1}^{N} \sum_{c=1}^{3} w_i^c y_i^c \log \hat{y}_i^c$$

Here, the probability of ground truth is represented by y_i^c, while byci gives prognosticated the probability of volume pixels i belonging a certain class-c (background, brain tumor) & the weighting factor of each class is represented by w_i^c. (Alalwan et al., 2021)

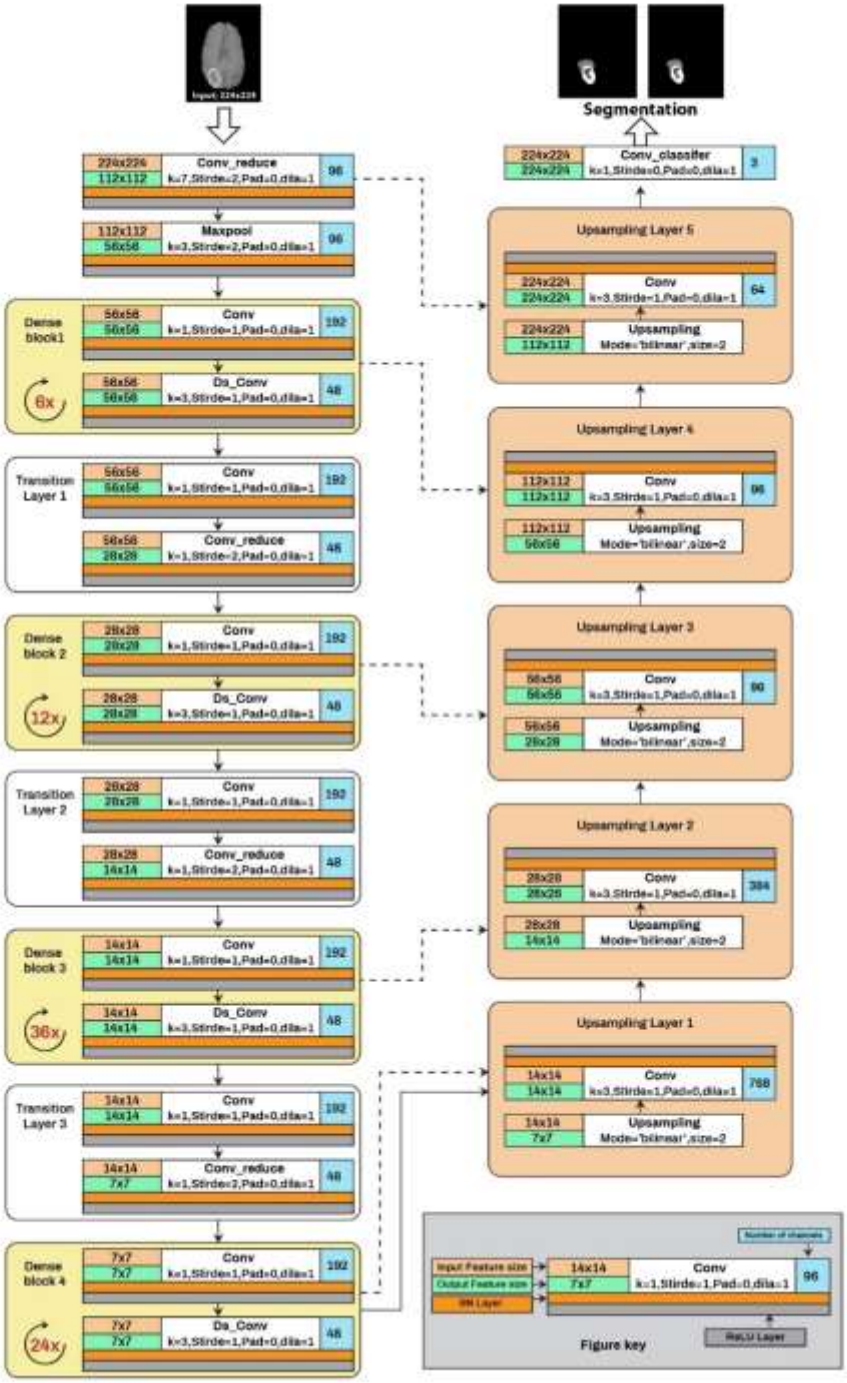

Figure 2. Semantic Brain & Tumor Segmentation using the proposed DSDU-Net Framework.

4. Experiments and Results

The experiments and model validation was carried out in a Python environment, utilizing keras, TensorFlow as a backend and implemented using Googlecolaboratory with specified data.

4.1.Performance Evaluation Metrics

The Designed network is validated using training&validation database. Evaluation results used include Hausdorfdistance , DiceScore, specificity&sensitivity for WT, TC, and ET. These are defined below:

4.1.1.Dice Similarity Coefficient.

Performance of semantic segmentation is typically evaluated using Dice score (Dice) or Dice Similarity Coefficient. It is the extent to which provided ground truth (GT) and the predicted masks (PM) overlap spatially. The mathematical definition is as follows:

$$Dice = \frac{2|GT \cap PM|}{|GT|+|PM|} * 100 \ldots\ldots\ldots\ldots\ldots\ldots\ldots(1)$$

Dice score values typically range from 0 to 100, with 100 being complete agreement and 0 overlapping.

4.1.2. Hausdorf Distance (95%)

Evaluation with spatial overlap agreement parameters alone for volumetric segmentation is not sufficient. Differences in slotted edges may not have a profound effect on the spatial overlap but may have a significant impact in areas close to the brain's boundaries, thereby leading to the presence of the skull or an omission of tumor regions. To combat this, we also use the 95th percentile of the Hausdorf f_{95} distance for evaluating maximum contour distance d between ground truth and predicted masks on a radial assessment.

$$Hausdorf\ f_{95} = percentile\ (d_{PM,GT} \cup d_{GT,PM}, 95^{th})$$

Higher Dice scores and lower Hausdorf f_{95} scores indicate enhanced results.

4.1.2 Sensitivity and Specificity

Sensitivity and specificity have also been taken into consideration as evaluation metrics. They are represented mathematically as follows.

$$Senitivity(P,T) = \frac{\left|P_1 \wedge T_1\right|}{|T_1|}$$

$$Specificity(P,T) = \frac{|P_0 \wedge T_0|}{|T_0|}$$

where P denotes the algorithm's prediction map, and T denotes the ground truth label fragmented manually by specialists. |•| represents no. of volume pixels set, P0, P1 denotes negative&positive volume pixels of predicted map, and T0, T1 denotes the negative&positive volume pixels of ground truth map.

4.2.Comparison with Existing Methods

Table 1: Compared With Existing Methods Based On Validation Dataset (Brats2018)

Table 1 (a): Comparison based on sensitivity and specificity

Reference	**Sensitivity**			**Specificity**		
	TumorCore	EnhancingTumor	WholeTumor	TumorCore	Enhancing Tumor	WholeTumor
(Myronenko, 2019)	0.865	0.847	0.926	0.998	0.998	0.995
(Isensee et al., 2019)	0.846	0.830	0.920	0.999	0.998	0.995

(McKinley et al., 2019)	0.836	0.830	0.913	0.998	0.998	0.994
(Zhou et al., 2019)	0.868	0.813	0.914	0.997	0.998	0.995
(Banerjee & Mitra, 2020)	0.873	0.869	0.913	0.997	0.997	0.993
Proposed Model	**0.889**	**0.872**	**0.926**	**0.999**	**0.999**	**0.999**

Table 1(b): Comparison predicated on Hausdorff Distance and Dice score

Reference	**Dice Score**			**Hausdorff Distance**		
	Tumorcore	Enhancing tumor	Wholetumor	Tumorcore	Enhancingtumor	Wholetumor
(Myronenko, 2019)	0.8155	0.7665	0.8840	4.8100	3.7732	5.9045
(Isensee et al., 2019)	0.863	0.809	0.913	6.518	2.413	4.268
(McKinley et al., 2019)	0.847	0.792	0.901	4.988	3.603	4.063
(Zhou et al., 2019)	0.8651	0.8136	0.9095	6.545	2.716	4.172
(Luo et al., 2021)	0.843	0.815	0.890	8.76	2.42	4.59
(Banerjee & Mitra, 2020)	0.872	0.8244	0.9724	5.061	2.636	4.748
Proposed model	**0.897**	**0.858**	**0.918**	**3.720**	**4.568**	**4.568**

Table 2: Compared With Existing Methods Based On Validation Dataset (BRATS2019)

Table 2(a): Comparison based on sensitivity and specificity

Reference	**Sensitivity**			**Specificity**		
	Tumorcore	Enhancingtumor	Whole Tumor.	Tumorcore	Enhancing tumor	Wholetumor
(Ali Hassen et al., 2021)	0.831	0.765	0.924	0.997	0.998	0.994
(Chen et al., 2020)	0.8027	0.7564	0.8655	0.9944	0.9981	0.9914
(Hamghalam et al., 2020)	0.826	0.766	0.897	0.996	0.998	0.995
(Li et al., 2020)	0.819	0.802	0.921	0.997	0.998	0.992

(Bakas et al., 2018)	77.71	76.88	91.32	99.76	99.85	99.39
Proposed Model	**0.834**	**0.859**	**0.897**	**0.999**	**0.998**	**0.999**

Table 2(b): Comparison predicated on Hausdorff Distance and Dice score

Reference	**Dice Score**			**Hausdorff Distance**		
	Tumorcore	Enhancing tumor	Wholetumor	Tumorcore	Enhancing tumor	Wholetumor
(Pei et al., 2020b)	0.835	0.821	0.895	6.712	3.319	4.897
(Jiang et al., 2020)	0.837	0.833	0.888	4.13	2.65	4.619
(Feng et al., 2020)	0.831	0.795	0.912	6.53	3.97	3.786
(Ali Hassen et al., 2021)	0.851	0.760	0.936	7.357	3.401	7.35
(Alshehhi & Alshehhi, 2021)	0.82	0.77	0.89	5.21	4.11	5.01
Proposed Model	**0.909**	**0.863**	**0.918**	**2.732**	**3.677**	**3.677**

Table 3. Comparison of supervised learning for tumorsubregions analysis based on dicescore & sensitivity

MODEL	**DiceScore**			**Sensitivity**		
	Tumorcore	Enhancing tumor	Whole tumor	Tumorcore	Enhancing tumor	Wholetumor
NoNew-Net (Isensee et al., 2019)	0.863	0.809	0.913	0.846	0.830	0.920
AMPNet (Chen et al., 2020)	0.7948	0.7413	0.893	0.7144	0.6813	0.8533
3D-UNET (Wang et al., 2020)	0.807	0.737	0.894	0.826	0.766	0.897
Two Step U-NET (Kim et al., 2020)	0.764	0.672	0.876	0.765	0.763	0.887
Proposed Model	**0.897**	**0.858**	**0.918**	**0.889**	**0.872**	**0.926**

5. Discussion

Segmentation of brain tumors into their subregions has been done performed with the help of deep learning models. The model has been trained with two datasets- The braTS 2018&2019 database that consists of 285 and 355 magnetic resonance images from patients with glioma. T1, T2, T1c, and T2 FLAIR are the four imaging modalities used in this dataset. Images are accessible in three different views: axial, coronal, and sagittal. Imaging methods in the axial view are among them is considered for the experiments. Figure -- shows the MRI of five random patients with the tumor sub-regions extracted. Images a-d depict the four different modalities, T1, T2, FLAIR, and T1c.

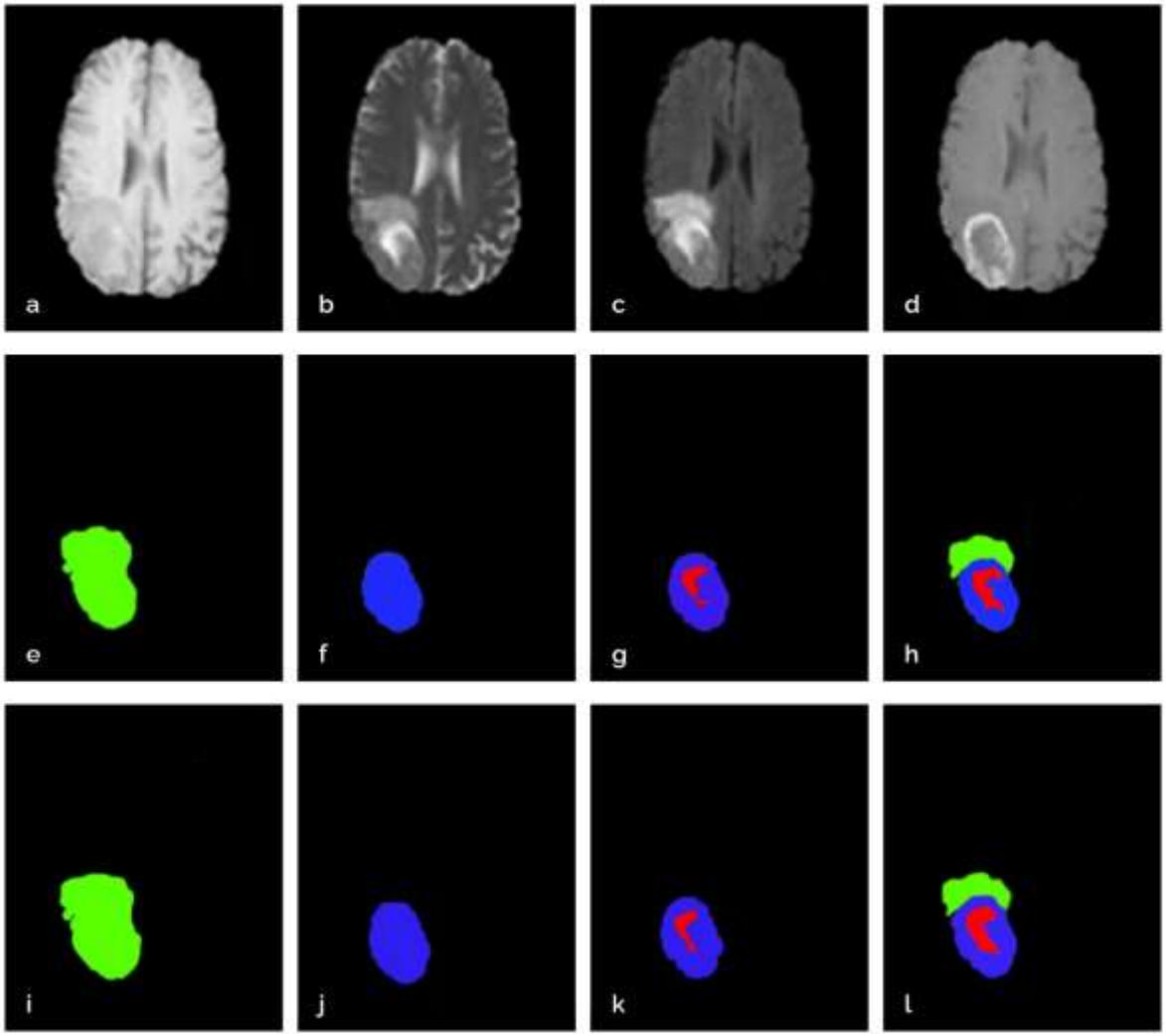

Fig. 3: Patient name segmentation for a brain tumor Deep learning models are used by Brats18 2013 3 1. T1 image, T2 FLAIR image, T1-contrast image are shown in the first row; ground truths of WT, TC, ET and all sub-regions combination are shown in the second row e–h; prediction of WT , TC, ET , all sub-regions combination (all) is shown in the third row i– l (All).

The model was evaluated from the subregions extracted from 10 random patients. Different evaluation metrics were used for analyzing the performance, and exemplary results were obtained. The performance metrics used for evaluation are the Hausdorfdistance and

Dicesimilarity coefficient; to measure structural overlap and sensitivity and specificity. Table 4 (a). shows performance metrics such as specificity and sensitivity applied to this model. The model has a specificity of 0.999 and a sensitivity of 0.9115. These results show that the model has outperformed most other models with a lesser number of false negatives in the prediction phase. From Table4(b).Hausdorff Distance & Dicecoefficient have been used to calculate structural overlap similarity of the sub-regions of brain tumors in MRI. Outcomes obtained proves that values are almost the same as the ground truth with average dicescores - 0.903, 0.8605, & 0.918 also average Hausdorff Distance were 3.226, 4.1225, & 4.1225. The results can help doctors, and radiologists detect features like position, shape and dimensions of brain tumor subregions.

Table 4 (a). Proposed DSDU-Net Tumor subregions Analysis

Evaluation Metric	DSDU-NET		
	TumorCore	EnhancingTumor	WholeTumor
Specificity	0.999	0.9985	0.999
Sensitivity	0.8615	0.8655	0.9115

Table 4(b). Proposed DSDU-Net Tumor subregions Analysis

Structural Overlap Similarity Metrics	DSDU-NET		
	TumorCore	EnhancingTumor	Whole Tumor
Dicesimilarity coefficient	0.903	0.8605	0.918
Hausdorff Distance	3.226	4.1225	4.1225

6. Conclusion & Future work

This study proposed using a depthwise separable convolutional network and a DSDU-NET segmenting tumor into Wholetumor (WT), Tumorcore(TC), and Enhancing tumor(ET). Several efficient methods have been used for pre-processing. Metrics like sensitivity, specificity, Hausdorff distance, and dice coefficient were evaluated. The model can also be used to dissection other tissues such as necrosis and cysts that are commonly seen with brain tumors. Enhanced longitudinal segmentation of tumors may be done with the help of a better label fusion method. The underlying methods for feature extraction can be enhanced further, and the amalgamation of a model that considers the treatment modality is an exciting area of research.

Funding Information

No funds, grants, or other support was received.

Ethics Approval

Not applicable

Conflicts of Interest

None.

Declaration of interests

The authors declare that they have no known competing financial interests or personal relationships that could have appeared to influence the work reported in this paper.

References

[1] Alalwan, N., Abozeid, A., ElHabshy, A. A. A., & Alzahrani, A. (2021). Efficient 3D deep learning model for medical image semantic segmentation. Alexandria Engineering Journal, 60(1), 1231–1239. https://doi.org/10.1016/j.aej.2020.10.046.

[2] Ali Hassen, O., Omar Abter, S., A. Abdulhussein, A., M. Darwish, S., M. Ibrahim, Y., & Sheta, W. (2021). Nature-inspired level set segmentation model for 3D-MRI brain tumor detection. Computers, Materials & Continua, 68(1), 961–981. https://doi.org/10.32604/cmc.2021.014404.

[3] Almezhghwi, K., Serte, S., & Al-Turjman, F. (2021). Convolutional neural networks for the classification of chest X-rays in the IOT ERA. Multimedia Tools and Applications, 80(19), 29051–29065. https://doi.org/10.1007/s11042-021-10907-y.

[4] Alshehhi, R., & Alshehhi, A. (2021). Quantification of uncertainty in brain tumor segmentation using Generative Network and Bayesian Active Learning. Proceedings of the 16th International Joint Conference on Computer Vision, Imaging and Computer Graphics Theory and Applications. https://doi.org/10.5220/0010341007010709.

[5] Bacanin, N., Bezdan, T., Venkatachalam, K., & Al-Turjman, F. (2021). Optimized convolutional neural network by Firefly algorithm for Magnetic Resonance Image Classification of Glioma Brain Tumor Grade. Journal of Real-Time Image Processing, 18(4), 1085–1098. https://doi.org/10.1007/s11554-021-01106-x.

[6] Bakas, S., Reyes, M., Jakab, A., Bauer, S., Rempfler, M., Crimi, A., Shinohara, R. T., et al. Identifying the Best Machine Learning Algorithms for Brain Tumor Segmentation, Progression Assessment, and Overall Survival Prediction in the BRATS Challenge. https://doi.org/10.17863/CAM.38755.

[7] Banerjee, S., & Mitra, S. (2020). Novel volumetric sub-region segmentation in brain tumors. Frontiers in Computational Neuroscience, 14. https://doi.org/10.3389/fncom.2020.00003.

[8] Chen, M., Wu, Y., & Wu, J. (2020). Aggregating multi-scale prediction based on 3D U-net in brain tumor segmentation. Brainlesion: Glioma, Multiple Sclerosis, Stroke and Traumatic Brain Injuries, 142–152. https://doi.org/10.1007/978-3-030-46640-4_14

[9] Díaz-Pernas, F. J., Martínez-Zarzuela, M., Antón-Rodríguez, M., & González-Ortega, D. (2021). A deep learning approach for Brain Tumor Classification and segmentation using a multiscale convolutional neural network. Healthcare, 9(2), 153. https://doi.org/10.3390/healthcare9020153.

[10] Feng, X., Tustison, N. J., Patel, S. H., & Meyer, C. H. (2020). Brain tumor segmentation using an ensemble of 3D U-Nets and overall survival prediction using radiomic features. Frontiers in Computational Neuroscience, 14. https://doi.org/10.3389/fncom.2020.00025.

[11] Hamghalam, M., Lei, B., & Wang, T. (2020). Convolutional 3D to 2D patch conversion for pixel-wise glioma segmentation in MRI scans. Brainlesion: Glioma, Multiple

Sclerosis, Stroke and Traumatic Brain Injuries, 3–12. https://doi.org/10.1007/978-3-030-46640-4_1.

[12] Isensee, F., Kickingereder, P., Wick, W., Bendszus, M., & Maier-Hein, K. H. (2019). No new-net. In A. Crimi, T. van Walsum, S. Bakas, F. Keyvan, M. Reyes, & H. Kuijf (Eds.), Brainlesion: Glioma, Multiple Sclerosis, Stroke and Traumatic Brain Injuries - 4th International Workshop, BrainLes 2018, Held in Conjunction with MICCAI 2018, Revised Selected Papers (pp. 234-244). (Lecture Notes in Computer Science (including subseries Lecture Notes in Artificial Intelligence and Lecture Notes in Bioinformatics); Vol. 11384 LNCS). Springer Verlag. https://doi.org/10.1007/978-3-030-11726-9_21.

[13] Jiang, Z., Ding, C., Liu, M., & Tao, D. (2020). Two-stage cascaded U-Net: 1st place solution to brats challenge 2019 segmentation task. Brainlesion: Glioma, Multiple Sclerosis, Stroke and Traumatic Brain Injuries, 231–241. https://doi.org/10.1007/978-3-030-46640-4_22.

[14] Kim, S., Luna, M., Chikontwe, P., & Park, S. H. (2020). Two-step U-nets for brain tumor segmentation and random forest with radiomics for survival time prediction. Brainlesion: Glioma, Multiple Sclerosis, Stroke and Traumatic Brain Injuries, 200–209. https://doi.org/10.1007/978-3-030-46640-4_19.

[15] Li, X., Luo, G., & Wang, K. (2020). Multi-step cascaded networks for Brain Tumor Segmentation. Brainlesion: Glioma, Multiple Sclerosis, Stroke and Traumatic Brain Injuries, 163–173. https://doi.org/10.1007/978-3-030-46640-4_16.

[16] Luo, Z., Jia, Z., Yuan, Z., & Peng, J. (2021). HDC-net: Hierarchical decoupled convolution network for Brain Tumor Segmentation. IEEE Journal of Biomedical and Health Informatics, 25(3), 737–745. https://doi.org/10.1109/jbhi.2020.2998146.

[17] McKinley, R., Meier, R., & Wiest, R. (2019). Ensembles of densely-connected cnns with label-uncertainty for Brain tumor segmentation. Brainlesion: Glioma, Multiple Sclerosis, Stroke and Traumatic Brain Injuries, 456–465. https://doi.org/10.1007/978-3-030-11726-9_40.

[18] Myronenko, A. (2019). 3D MRI brain tumor segmentation using Autoencoder regularization. Brainlesion: Glioma, Multiple Sclerosis, Stroke and Traumatic Brain Injuries, 311–320. https://doi.org/10.1007/978-3-030-11726-9_28.

[19] Naser, M. A., & Deen, M. J. (2020). Brain tumor segmentation and grading of lower-grade glioma using deep learning in MRI images. Computers in Biology and Medicine, 121, 103758. https://doi.org/10.1016/j.compbiomed.2020.103758.

[20] Nassar, S., Mohamed, M., & Elnakib, A. (2021). MRI brain tumor segmentation using deep learning. (dept. E). MEJ. Mansoura Engineering Journal, 45(4), 45–54. https://doi.org/10.21608/bfemu.2021.139470.

[21] Pei, L., Bakas, S., Vossough, A., Reza, S. M. S., Davatzikos, C., & Iftekharuddin, K. M. (2020). Longitudinal brain tumor segmentation prediction in MRI using feature and label fusion. Biomedical Signal Processing and Control, 55, 101648. https://doi.org/10.1016/j.bspc.2019.101648.

[22] Pei, L., Vidyaratne, L., Rahman, M. M., & Iftekharuddin, K. M. (2020). Context aware deep learning for brain tumor segmentation, subtype classification, and survival prediction using Radiology Images. Scientific Reports, 10(1). https://doi.org/10.1038/s41598-020-74419-9.

[23] Peng, S., Chen, W., Sun, J., & Liu, B. (2019). Multi-scale 3D U-NETS: An approach to automatic segmentation of brain tumor. International Journal of Imaging Systems and Technology, 30(1), 5–17. https://doi.org/10.1002/ima.22368.

[24] Serte, S., Serener, A., & Al-Turjman, F. (2020). Deep Learning in Medical Imaging: A brief review. Transactions on Emerging Telecommunications Technologies. https://doi.org/10.1002/ett.4080.

[25] Wang, F., Jiang, R., Zheng, L., Meng, C., & Biswal, B. (2020). 3D U-Net based brain tumor segmentation and survival days prediction. Brainlesion: Glioma, Multiple Sclerosis, Stroke and Traumatic Brain Injuries, 131–141. https://doi.org/10.1007/978-3-030-46640-4_13.

[26] Wu, W., Li, D., Du, J., Gao, X., Gu, W., Zhao, F., Feng, X. & Yan, H., 2020. An Intelligent Diagnosis Method of Brain MRI Tumor Segmentation Using Deep Convolutional Neural Network and SVM Algorithm. Computational and Mathematical Methods in Medicine, 2020.

[27] Zawish, M., Ali, A., Hyder, S., Zahid, A., & Khalil, A. (2019). Brain tumor segmentation through region-based, supervised and unsupervised learning methods: A literature survey brain tumor segmentation through image processing methods: A literature survey. Journal of Biomedical Engineering and Medical Imaging, 6(2). https://doi.org/10.14738/jbemi.62.6725 .

[28] Zhao, Y.-X., Zhang, Y.-M., & Liu, C.-L. (2020). Bag of tricks for 3D MRI brain tumor segmentation. Brainlesion: Glioma, Multiple Sclerosis, Stroke and Traumatic Brain Injuries, 210–220. https://doi.org/10.1007/978-3-030-46640-4_20.

[29] Zhou, C., Chen, S., Ding, C., & Tao, D. (2019). Learning contextual and attentive information for Brain Tumor Segmentation. Brainlesion: Glioma, Multiple Sclerosis, Stroke and Traumatic Brain Injuries, 497–507. https://doi.org/10.1007/978-3-030-11726-9_44 .